Study of cLFV decays in $b\bar{b}$ at Belle II

Ravinder Dhayal

A dissertation submitted for the partial fulfilment of

BS-MS dual degree in Science

Indian Institute of Science Education and Research Mohali

June 2020

Dedicated to my Family

Certificate of Examination

This is to certify that the dissertation titled **"Study of cLFV decays in $b\bar{b}$ at Belle II "** submitted by **Ravinder Dhayal** (Reg. No. MS15068) for the partial fulfillment of BS-MS dual degree programme of the Institute, has been examined by the thesis committee duly appointed by the Institute. The committee finds the work done by the candidate satisfactory and recommends that the report be accepted.

Dr. Ambresh Shivaji Dr. Aru Beri Dr. Vishal Bhardwaj
(Supervisor)

Dated: June 30, 2020

Declaration

The work presented in this dissertation has been carried out by me under the guidance of Dr.Vishal Bhardwaj at the Indian Institute of Science Education and Research Mohali.

This work has not been submitted in part or in full for a degree, a diploma, or a fellowship to any other university or institute. Whenever contributions of others are involved, every effort is made to indicate this clearly, with due acknowledgement of collaborative research and discussions. This thesis is a bonafide record of original work done by me and all sources listed within have been detailed in the bibliography.

Ravinder Dhayal
(Candidate)

Dated: June 30, 2020

In my capacity as the supervisor of the candidate's project work, I certify that the above statements by the candidate are true to the best of my knowledge.

Dr. Vishal Bhardwaj
(Supervisor)

Acknowledgment

Firstly, I would like to express my sincere gratitude towards my supervisor Dr. Vishal Bhardwaj for his kind support, guidance, motivation and the immense knowledge. Without his help and guidance, the project would not have been possible. I am very thankful to him for giving me an opportunity to work under his guidance.

Besides my advisor, I would like to thank the rest of my thesis committee members Dr.Ambresh Shivaji, and Dr.Aru Beri for their insightful comments and encouragement.
I sincerely thank Belle II Collaboration for providing me necessary computing tools and resources.

I want to thank all my seniors and group members for supporting and helping me during the entire period of the project, especially Debjit Ghosh, Rajesh Maiti, Renu Garg, Sourav Patra for assisting me with discussions.

I also want to thank Adeeb Mev, Ajay, Dharm Singh, Jasmeet Singh and Rajesh Bajiya for making this journey an enjoyable one, including their late night music sessions and life lessons. I also want to thank my other friends, Jaspreet Kaur, Shivali Sokhi and Sunil Dahiya. I must express my very profound gratitude to Pooja Dhayal and Hunar for providing me personal and professional support. This accomplishment would not have been possible without them.
A special mention and thanks to Aashke, my Bhangra team for being an important part of my life and for all the great memories through these years.

I acknowledge IISER Mohali for providing me best Infrastructures and environment for carrying out this project. I am also thankful to the "Department of Science and Technology," Govt. of India for supporting me with institute fellowship during the past five years.

To conclude above all, it was almighty and my family which have been there all these years strongly supporting and guiding me in life.

List of Figures

List of Tables

Notation and Abbreviations

B	B meson
e^-	Electron
e^+	Positron
$\Upsilon(2S)$	Upsilon(2S)
$\Upsilon(1S)$	Upsilon(1S)
μ^+	Muon
μ^-	Anti-muon
ν	Neutrino
$\bar{\nu}$	Anti-neutrino
π^+	Pion
π^-	Anti-pion
τ^+	Tau
τ^-	Anti-tau

Contents

Abstract

The Belle II experiment at the SuperKEKB is an electron positron collider that produces an instantaneous luminosity of $8 \times 10^{35}\ cm^{-2}\ s^{-1}$ and the experiment is expected to accumulate a data sample of about 50 ab^{-1}. With this amount of data, decays sensitive to physics beyond the Standard Model can be studied with unprecedented precision.

In the search for Charged Lepton Flavor Violation (cLFV) in bottomonium ($b\bar{b}$) decays, we look through 1 million events for $\Upsilon(2S)$ sample simulated through the Belle II detector. Now for cLFV transition, $\Upsilon(1S)$ has been studied in $\Upsilon(2S) \rightarrow \pi^+\pi^-\Upsilon(1S)[\rightarrow \tau^+\tau^-], \tau^{\pm} \rightarrow \pi\pi\pi\nu$ and $\pi\pi\nu$ decays. The presence of neutrinos in the above decay chain makes it difficult to reconstruct full signal and results in large background. We need proper methods to reduce the background and identify the signal. The aim of this project was to do so and perform sensitives study.

Chapter 1

Introduction

Theories and discoveries, in an attempt to explain the physical world and it's principles at a fundamental level, have been through decades of vigorous research. As a result, we today have a remarkable understanding of the fundamental structure of matter, fundamental forces and particles that constitute it. Our current knowledge of Particle physics, based on experimental observations and theoretical predictions is described through the Standard Model (SM).

1.1 The Standard Model of Particle Physics

The Standard Model of Particle Physics (SM), formulated through the shared efforts of many scientists and finalised in the 1970s, has achieved monumental success since its conception. Standard Model describes the existence of fundamental particles and the nature of their interactions. Other than the subatomic particles, SM was successful in predicting the existence of additional particles years before their discoveries, some of them being the top quark (discovered in 1995), the tau neutrino (discovered in 2000) and the Higgs Boson in 2012 being the most recent of them.

SM consists of elementary particles grouped into two classes: Bosons (with spin either 0, 1 or 2) and Fermions (with spin 1/2). Fermions make up the matter while bosons transmit forces within the matter. The fermions are further classified into Leptons and Quarks. The known leptons and quarks are grouped into three generations. Figure 1.1 provides an overview of each particle incorporated within the SM

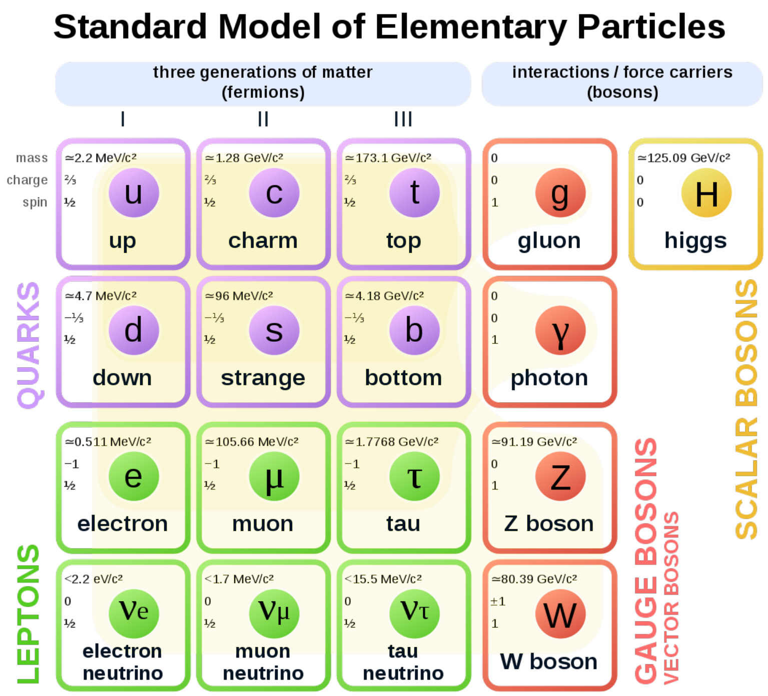

Figure 1.1: The Standard Model

SM also includes five bosons, which are, four types of gauge bosons with spin 1, and the Higgs boson which possesses a spin of 0. The gauge bosons are the force-carrying particles responsible for the fundamental interactions between SM particles, specifically the electromagnetic, strong, and weak forces. The gravitational force is also considered to be fundamental in nature, though it is not incorporated into the SM and has no associated gauge boson within the model.
Even though the SM is quite successful to explain the existence of matter around us, there are many places where it fails. One of such examples is the CP violation (necessary for matter-antimatter asymmetry) which is by product of CKM mechanism in the SM, but this produces very less asymmetry. One can not thus explain the large asymmetry as observed in the universe. Further, neutrino oscillations, dark matter and dark energy are few of the mysteries which are not explained by the SM. This suggests the need to go beyond the SM and need of some other mechanism (generically known as New Physics beyond the SM).

Many particle collider experiments are also actively involved in the global search for new physics, investigating particle decays for any significant deviations from SM predictions. The Belle II Experiment located in Tsukuba, Japan, is one such collaboration, with the primary aim of using rare B-meson decays to search for New Physics signatures .

1.2 Meson

Quarks are known to bind into triplets and doublets. The doublets formed by quark-anti-quark pairs are known as Mesons while the triplets are called Baryons. Collectively, baryons, mesons and quarks are knows as Hadrons. Mesons are bosons (have integer spin), while baryons are fermions (have half-integer spin). Causes formed from the quarks, mesons can participate in both strong and weak interactions. Due to the lighter weight (compared to baryons), they are more easily produced in the experiments.

The classification of mesons is done according to their quark content, total angular momentum, parity, etc. Spin represents the intrinsic angular momentum of a particle. There are two possible conditions for the alignment of quarks, when their spins are aligned, the spin vectors add up to make a vector of length S = 1 with three spin projections (S_z= +1 , S_z = 0 and S_z = 1) called the spin-1 triplet. The spins when unaligned add up and result in a vector of length S = 0, and spin projection (S_z =0) called spin-0 singlet. Mesons can form both triplet and singlet spin states.

1.2.1 Bottomonium ($b\bar{b}$) & $\Upsilon(2S)$

Bottomonium is the system consisting of a b and $\bar{b}$ quark bound by the strong force. The heavy b quark mass allows this system to be described by nonrelativistic field theory, in addition to phenomenological and lattice methods. e^+e^- colliders can directly produce excited bottomonium states, Υ. The Υ mesons are the bound state of the $b\bar{b}$ and mesons were confirmed by experiments at CESR and DORIS. The width of $\Upsilon(4S)$ resonance is significantly larger than the width of the three lighter resonances $\Upsilon(1S), \Upsilon(2S), \Upsilon(3S)$. In this thesis we will mainly focus on $\Upsilon(1S)$ and $\Upsilon(2S)$.

Meson	Mass(MeV/c^2)	Total width(MeV)
$\Upsilon(1S)$	9460.30 $\pm$0.26	0.05402 $\pm$0.00125
$\Upsilon(2S)$	10023.26 $\pm$0.31	0.03198 $\pm$0.00263
$\Upsilon(3S)$	10355.2 $\pm$0.5	0.02032 $\pm$0.00185
$\Upsilon(4S)$	10579.4 $\pm$1.2	20.5 $\pm$2.5

Table 1.1: Masses (MeV/c^2) & widths (MeV) of Υ mesons.

1.3 Lepton Number Conservation & cLFV

Lepton Number conservation states that the sum of lepton numbers before and after the interaction must remain conserved. If we assign lepton number L$= +1$ to leptons, L $= 1$ to antileptons, and L $= 0$ to all other particles we find that the net lepton number of all particles going into an interaction equals the net lepton number of all particles coming out of the interaction. In other words the net lepton number of the system is unchanged by the interaction. The conservation of lepton number is one of the accidental symmetries of the Standard Model. However, the observation of neutrino mixing suggests that charged lepton flavour violation should exist.

1.3.1 Charged Lepton Flavor Violation (cLFV)

According to SM, each of the three generations of leptons should have its own conserved lepton number. Charged lepton flavor violation (cLFV) necessitates the mixing of the generation between leptons.
Neutrino Oscillation (discovered in 1988 by the Super-Kamiokande experiment) [Nakamura 18] is caused by the finite but very small mass of neutrinos. The atmospheric muon neutrinos generated by the collision between cosmic rays and the atmosphere on the earth were observed muon in Super-Kamiokande, the number of the upward going neutrinos was only half of the number of the down going neutrinos. This finite small mass of neutrino leads to cLFV but with suppression ($\sim 10^{-54}$ or so). However, NP can accelerate the cLFV decay leading to its higher branching fraction. By searching for cLFV, one can look for the NP cases.

A summary of already published results on the search for cLFV in Υ(nS)[n =

$1, 2, 3]$ decays by CLEO and BaBar is shown in Table 1.2. [S. Patra 0]

Search for the decay	Experiment	Upper bound
$\Upsilon(1S) \to \mu\tau$	CLEO	$< 6.0 \times 10^{-6}$ (95%)
$\Upsilon(2S) \to \mu\tau$	CLEO	$< 14.4 \times 10^{-6}$ (95%)
$\Upsilon(2S) \to e\tau$	BaBar	$< 3.2 \times 10^{-6}$ (90%)
$\Upsilon(3S) \to \mu\tau$	CLEO	$< 26.3 \times 10^{-6}$ (95%)
$\Upsilon(3S) \to e\tau$	BaBar	$< 4.2 \times 10^{-6}$ (90%)
$\Upsilon(3S) \to \mu\tau$	BaBar	$< 3.1 \times 10^{-6}$ (90%)

Table 1.2: Previously published results on the cLFV [S. Patra 0]

We also looked at the reconstruction of $\Upsilon(1S) \to \tau^+\tau^-$, as the PDG uses results with less data in comparison to what we have in Belle. This study was aimed to bring ideas one can use to study possible tau reconstruction in order to recover the Upsilon decays (where it has one tau and therefore missing neutrino).

Chapter 2

The Belle II Experiment

The journey of the Belle and Belle II started in 1999 from Tsukuba, Japan. The Belle experiment made important discoveries on flavor structure of elementary particles, CP Symmetry Violation. The Belle II experiment uses the SuperKEKB particle collider (an upgrade to the KEKB collider at Belle) which aims to explore the decay of B mesons formed by the collision of electron and positron at the center of mass energy of $\Upsilon(4S)$.

This chapter gives a brief introduction of the Belle II accelerator and detectors and also provides an overview of `basf2` software which is provided by KEK server for the computation.

2.1 Accelerator

SuperKEKB uses similar two rings to that used by KEKB: a low-energy ring (LER) for positrons and a high-energy ring (HER) for electrons. In SuperKEKB the Nano-Beam scheme is used, where the idea is to minimize the longitudinal size of the overlap region of the two beams at the interaction point. The new beam energies have been changed from 3.5 and 8.0 GeV to 4.0 GeV and 7.0 GeV. In the interaction region, the 7 GeV electrons in the HER and the 4 GeV positrons in the LER collide at one interaction point (IP) with a non-zero crossing angle of 83 mrad.

2.2 Belle II Detector

The Belle II detector is given in the Fig. 2.1 with various subdetectors within it. The detector is configured within a 1.5 T superconducting solenoid and iron structure surrounding the SuperKEKB beams. Decay vertices are reconstructed by a pixelated silicon sensors (PXD) and a silicon vertex detector (SVD), situated just outside a cylindrical beryllium beam-pipe. A central drift chamber (CDC) provides principal charged particle monitoring. Particle identification is provided by dE/dx measurements in the CDC and time-of-propagation (TOP) counters. An array of CsI(Tl) crystals located within the solenoid coil detects electromagnetic showers. Muon and K_L mesons are identified by arrays of resistive plate counters (RPCs) interspersed in the iron yoke.

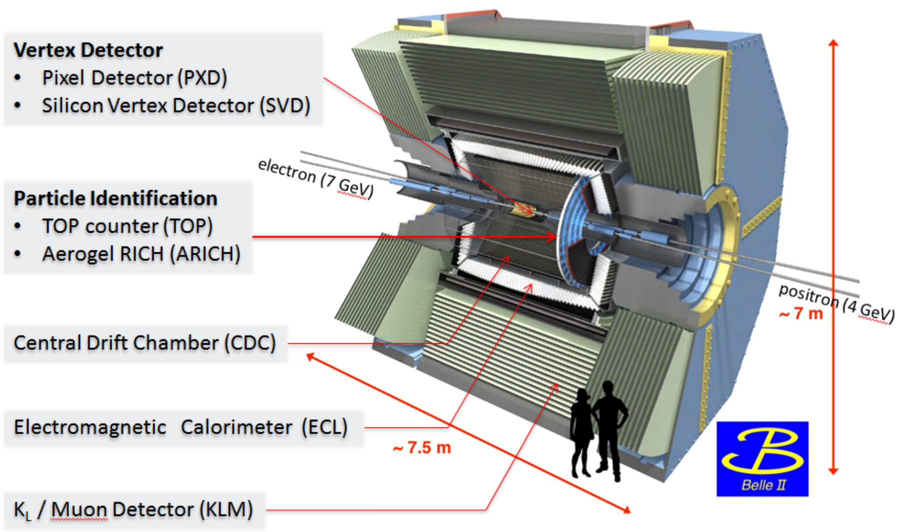

Figure 2.1: Belle II detector

The positive z-axis runs from the interaction point parallel to the electron beam trajectory; polar angle is the azimuthal angle from the z-axis. The detector is rotational symmetrical along the z-axis. The detector covers the polar angle from 17° to 150°, or about 93° of the solid angle.

2.2.1 Vertex Detector (VXD)

Vertex detectors consists of two detectors, one is silicon pixel detector (PXD), and the other is silicon strip detector (SVD) [Adachi 18]. The main purpose of the vertex detectors is tracking of the particles.

The PXD detector is two layers with layer 1 (L1) at radius 14 mm and layer 2 (L2) with radius 22mm. It is based on Depleted P-channel Field Effect Transistor (DEPFET) technology.

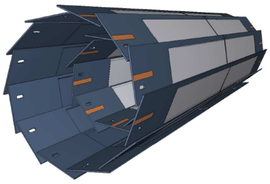

(a) Schematic view of PXD Detector

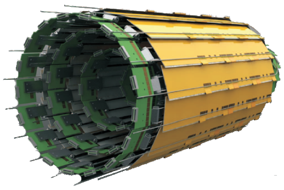

(b) Schematic view of PXD Detector

Figure 2.2: VXD Detector (Taken from [Li 15])

A DEPFET pixel consists of a fully depleted substratum and is equipped with a MOSFET p-channel structure and an internal gate where the electrons from the depleted substratum are collected within the minimum local electrical potential in the pixel.

The SVD detector is rectangular and trapezoidal and constitutes the four outer layers of VXD. It has four layers with double-sided silicon microstrip detectors (DSSDs) with sensor radii to 38, 80, 115, and 140 mm. Thus the VXD has total of six layers around the beam pipe. The total power consumption of the vertex detector is very high, and it is supported with proper cooling channels using $-20°$C liquid CO_2.

2.2.2 Central Drift Chamber (CDC)

In the Belle II detector, the central drift chamber (CDC) plays three important roles:

- Reconstructs the trajectories of charged particles and thus determines the momenta.

- Provides particle identification information using measurements of energy loss within its gas volume.

- Provides efficient and reliable trigger signals for charged particles.

It consists of a large volume gas drift chamber filled with Helium-Methane mixture with drift cells. The CDC cell is 1200 mm wide and 250 mm thick and consists of a lot of anode and cathode wires.

2.2.3 Particle Identification system (TOP and ARICH)

The time-of-propagation (TOP) counter is used for particle identification in the outer region of the CDC, and it uses the Cherenkov principle for the identification. This detector provides a separation between kaons and pions. In the end-cap region, a Cherenkov imaging detector ARICH with aerosol as a radiator is used to identify charged particles [Adachi 18].

2.2.4 Electromagnetic Calorimeter (ECL)

The purpose of electromagnetic calorimeter (ECL) is to detect γ rays (photons) which are not visible in the tracking detectors, and to measure their energy and position. The main tasks of the calorimeter are:

- Detection of photons with high efficiency,
- Precise determination of the photon energy and angular coordinates,
- Electron identification,
- Generation of the proper signal for trigger,
- On-line and off-line luminosity measurement, and
- K_L^0 detection together with the KLM.

It consists of a heavily-segmented array of Thallium-doped Cesium Iodide CsI(Tl) crystals and is located at the top end region and barrel region. It consists 8736 Tl-doped CsI scintillation crystals with a cross section of about 66 cm^2 and a length of 30 cm. In the crystals, photons are converted to electron-positron pairs, which in turn emit bremsstrahlung photons.

2.2.5 K_L/Muon Detector (KLM)

The KLM , used in K_L and muon detection, is the outermost detector portion at Belle II. Most of the electrons and photons produced in a collision do not reach the KLM the remaining particles are often muons or charged hadrons ($\pi^{\pm}$ or $K^{\pm}$). The KLM exists outside the detector's magnetic field and consists of an alternating sandwich of 4.7 cm thick iron plates, and active detector elements. As with the ECL, the KLM has barrel and end-cap components. It is used to provide a separation between hadrons and muons.

At Belle the active detector elements were glass-electrode resistive plate chambers (RPC). These elements have worsened efficiency under high background fluxes due to their long dead time; at Belle II the end-cap and innermost barrel RPCs have been replaced with scintillators.

2.3 Beam Backgrounds

Beam background is an important issue in B-factories. Sometimes beam particles are deviate from the ideal orbit and produce electromagnetic showers by hitting the wall of the beam pipe. If they are lost near the detectors, the resulting showers can hit the detectors. They are called beam background and the detectors are affected by fake hits and their associated radiation damage. Key sources of this beam background are Synchrotron radiation, beam-gas scattering, Touschek scattering, Luminosity backgrounds, Bremsstrahlung, Coulomb scattering etc. The axial magnetic field is 1.5 T and is provided by superconducting solenoid [Adachi 18]. The trigger system rejects the large background events coming from beam scattering and Bhabha scattering.

2.4 Luminosity

In SuperKEKB the collision takes place at 10.58 GeV which is center of mass energy of Υ(4S) resonance,

$$E_{CM} = 2\sqrt{E_{HER}E_{LER}} = 10.58GeV \sim M_{\Upsilon(4S)}$$

The expected luminosity will be 40 times higher than at KEKB, due to the higher beam currents and smaller interaction point beam sizes. At the interaction point, electrons and positrons undergo different types of interactions: Bhabha scattering, two-photon events, muon and tau pair production and quark pair production.

2.5 basf2 and gbasf2

Belle II analysis software framework (`basf2`) is a software written for Belle II experiment analysis [Kuhr 18]. It replaces the old `basf` which is provided for the computation in Belle experiment. The framework is primarily programmed using C++, but Python is the main language chosen for writing scripts that is executed by the framework. Other relevant external packages include `EvtGen`, used for the simulation of particle decays, particularly those of B and D mesons, and `Geant4`, responsible for simulating the interaction and consequent detection of particles by the various sub-detectors. Several other modules, packages that are useful in Belle II and are included in `basf2` are:

- Framework: modules relating to file input and output, Python steering and parallel processing.
- Geometry: modules relating to building the detector geometry for simulation.
- Simulation: modules relating to the generation of particle decay events and the simulation of their detection.
- Tracking: modules used for identifying particle tracks, and fitting tracks to decay vertices.
- Analysis: modules and libraries relevant for physics analyses, such as decay event reconstruction and event selections.
- MVA: modules used to perform multi-variate analysis, a machine learning technique.

The software is provided on the KEK computing work server. Different releases are available and are updated from time to time. It also allows submitting jobs at the Belle cluster where multiple jobs can be submitted at the same time.

Chapter 3

Analysis

3.1 Belle II Simulation

In this section we include a brief review of the simulation tools and the main event generators. All simulations start with at least one event generator that simulates the primary physics process, followed by a detailed detector simulation.

3.1.1 Generator

In this analysis, `EvtGen` is used to model the decays of B and D mesons into exclusive final states. `EvtGen` is an event generator originally developed for BaBar and CLEO. `EvtGen` accounts for cascade decays involving multiple vertices and spin configurations. In Belle II, `EvtGen` is controlled by means of a fairly complete decay table (DECAY.DEC), which lists all possible decay processes, their branching ratios, and the model (amplitude) which is to be used to decay them.

3.1.2 Detector Simulation

The simulation package of `basf2` is based on the `Geant4` software, with the version number 10.1.2.3. There are two methods to supply the primary event to `Geant4`: one can use the particle gun class, which is part of the `Geant4` package, or one can employ a specific generator software. We focus on the later case, the particles created by the generator package are sent to `Geant4` for simulation via the interface implemented in the `basf2` simulation package. Most of the decay processes of particles are described by the generator software. Short lived particles such as K_S^0 are usually decayed by `Geant4`. Exchange bosons and initial particles such as e^- and e^+ are not passed to `Geant4`. During the simulation, `Geant4` transports each primary particle step–by–step inside the detector and creates secondary particles. Digitisation of hit information in the sensitive volume of the detectors is handled by separate `basf2` modules, rather than using software objects incorporated into `Geant4`. The result from the `Geant4` simulation is sent to a persistent data storage (Data Store) to be used by other `basf2` modules.

3.2 Monte Carlo production

Electron-positron (e^-e^+) collisions at Belle II will produce a wide range of different physics events. Within these, we hope to find the various signal modes for our analysis. Each data analysis problem should be done on the proper data and it becomes more important when dealing with huge amount of data coming from experiments. However, a range of non-signal mode events are also produced; these events which are referred to as background (or sometimes physics background, distinct from beam-background) must be suppressed in order to effectively investigate signal processes. To check whether a data is important or not we apply selection criteria such as energy, momentum, angular relations and event shape variables. This criteria is optimised by examining Monte Carlo (MC) simulated signal and background events. MC events are produced using physics event generators and the response of the detector is simulated.

3.3 Reconstruction

Online and offline data handling is performed by the Belle II analysis software framework (`basf2`). The framework is designed to allow independent processing blocks called modules to perform relatively small tasks, which are executed linearly within a defined path. The configuration of modules for a specific purpose is defined using steering files. Modules communicate by passing information to and from a common object store, which also keeps track of relationships between objects in each event.

- **Particle identification (ID) variables**: In `basf2`, a particle ID exists for each charged final-state particle, namely the electronID, muonID, pionID, and kaonID. For all but the pionID, these variables represent the likelihood ratio that a particular charged track is in fact the named particle as opposed to a charged pion.

- **Track momentum variables**: These include the magnitude of the total momentum (p), as well as the individual transverse and z-components of the momentum, p_t and p_z respectively. These variables are useful for discriminating between tracks originating from different final-state particles with characteristic momentum distributions.

- **Invariant mass**: The difference between the invariant mass of the candidates and the established nominal mass, δM, is also used as classifier input for these intermediate particles, together with the invariant mass, M, of each daughter candidate.

3.4 Signal generation

3.4.1 Control sample

The electron-positron collision at SuperKEK takes place at the energy of 10.58 GeV which corresponds to the invariant mass of $\Upsilon(4S)$ thus all beam parameters are set on $\Upsilon(4S)$ region. However, in future one expect it to accumulate data at $\Upsilon(1S)$, $\Upsilon(2S)$, $\Upsilon(3S)$ and $\Upsilon(5S)$ for different physics cases. For our work we are interested in $\Upsilon(2S)$, for which we reset the beam energy by using payload. This was done by generating a database.txt file for $\Upsilon(2S)$ beam parameter and which was then used via payload in the `EvtGen` process. For control samples, we started with two decay channels which were then used to reconstruct $\Upsilon(2S)$ via $\Upsilon(1S)$ reconstruction. One million simulated signal events were generated for each control sample. For $\Upsilon(2S) \rightarrow \Upsilon(1S)\ \pi^+\pi^-$ decay we used VVPIPI model and for generating $\Upsilon(1S) \rightarrow ee/\mu\mu$ decays VLL model was used.

3.4.2 Particle Identification

Υ meson is reconstructed from its decay products. The particles used to reconstruct Υ meson are $e^{\pm}$, $\mu^{\pm}$, $\pi^{\pm}$. These are the final particles detected by the detector that are needed to reconstruct our decay mode of interest.

3.4.3 π/K selection

Charged K and π selection is based on the information from iTOP, ARICH and CDC sub-detectors. The pion (kaon) identification is based upon the likelihood ratio, which is defined as:

$$\mathcal{R}(\pi) = \frac{\mathcal{L}(\pi)}{\mathcal{L}(\pi) + \mathcal{L}(\mathcal{K})} \tag{3.1}$$

Charged pions (kaons) are identified by equiring the $\mathcal{R}(\pi) > 0.6$. $\mathcal{R}(\pi)$ distribution is shown in Fig. 3.1.

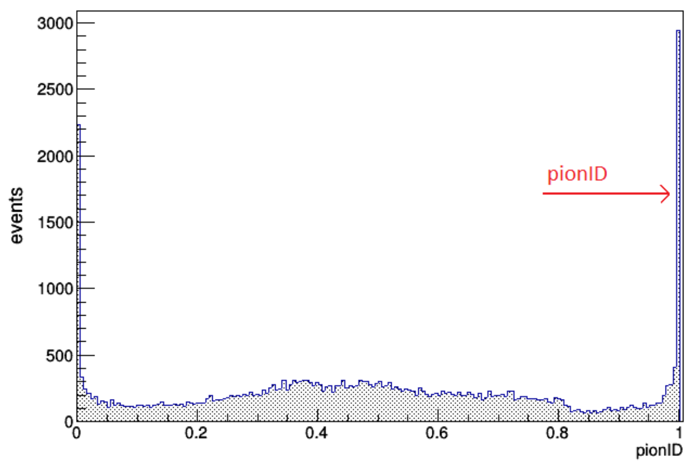

Figure 3.1: $\mathcal{R}(\pi)$ distribution with cuts used to identify π and K candidate .

3.4.4 Analysis strategy

We aim to reconstruct the signal for $\Upsilon(1S) \to \tau^+\tau^-$. However, as the first step we reconstructed the most straight forward decays $\Upsilon(1S) \to e^+e^-/\mu^+\mu^-$. This was done in order to verify our reconstruction process and to gain confidence in our particle selection criteria. $\Upsilon(1S) \to \ell^+\ell^-$ where ℓ stands for e or μ act as our control sample.

We look the recoil mass distribution of two pion ($M_{\pi\pi}^{recoil}$). We define our signal region variable as,

$$\Delta E = E_{\Upsilon(2S)}^{CM} - E_{beam} \tag{3.2}$$

$$M_{\pi\pi}^{recoil} = \sqrt{E_{CM}^2 + M_{\pi\pi}^2 - 2E_{CM}E_{\pi\pi}} \tag{3.3}$$

where $E_{\Upsilon(2S)}^{CM}$ is the centre-of-mass energy of the reconstructed $\Upsilon(2S)$, and E_{beam} is the total centre-of-mass energy of the electron-positron beam system, E_{cm}, $E_{\pi\pi}$ and $M_{\pi\pi}$ are total beam energy, total energy of two pion system and total mass of two pion system in $\Upsilon(2S)$ rest frame. In case of full reconstruction, we expect the ΔE to have value around 0. However, in case of a missing particle we can expect the peak in the negative region. When we calculate the Recoil mass, ideally $M_{\pi\pi}^{recoil}$ should peak at $\Upsilon(1S)$ mass.

3.5 Reconstruction

Using the identified final states, intermediate and primary states can be reconstructed. Reconstruction of events can be separated into three sections; tracking, calorimeter reconstruction, and particle identification. To reconstruct events in `basf2`, we start by filling lists of charged particles.

$\Upsilon(2S)$ and $\Upsilon(1S)$ are reconstructed using the following decay processes,

$$\Upsilon(2S) \to \Upsilon(1S)\pi^+\pi^-, \Upsilon(1S) \to e^+e^-, \mu^+\mu^- \tag{3.4}$$

$$\Upsilon(2S) \to \Upsilon(1S)\pi^+\pi^-, \Upsilon(1S) \to \tau^+\tau^-, \tau \to \pi\pi\pi\nu_\tau \tag{3.5}$$

For reconstruction we start from the control sample.

3.5.1 $\Upsilon(1S)$ from ee & $\mu\mu$

$\Upsilon(1S)$ is reconstructed from its decay particles e^+e^- and $\mu^+\mu^-$. Fig. 3.3 shows the reconstructed invariant mass of $\Upsilon(1S)$ for both cases. We select $\Upsilon(1S)$ mass from 9.0 to 9.7 GeV/c^2. In $\Upsilon(1S) \to e^+e^-$, we can expect energy loss by the electrons tracks in the form of bremsstrahlung photons. We tried to recover it by adding the γs shower in the 50 mrad direction of the electron track to the electron. However, even after this correction, the $\Upsilon(1S) \to e^+e^-$ signal shape is still skewed.

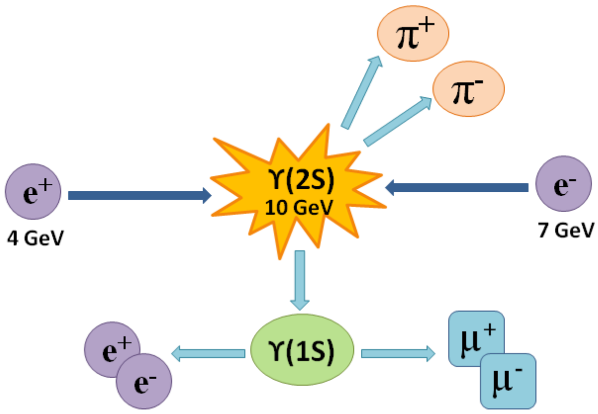

Figure 3.2: Schematic depicting the Decay process (3.4)

Here in Fig. 3.4 we plot the δM = M($\ell\ell$)$-$m$_{\Upsilon(1S)}$, where $M(m)$ is the invariant mass (nominal mass) of the reconstructed $\Upsilon(1S)$. For both of these cases, ee and $\mu\mu$, the observed peak is around 0.

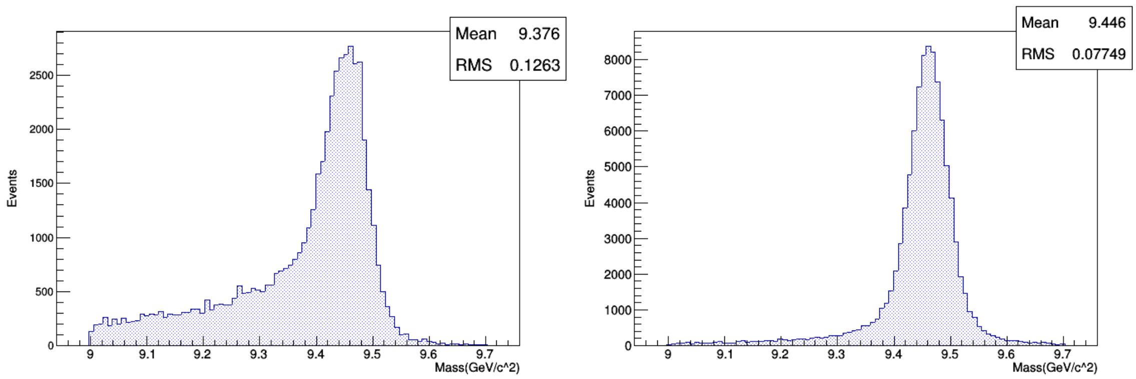

(a) $M(e^+e^-)$ of $\Upsilon(1S)$ in $\Upsilon(1S) \to e^+e^-$ decay.

(b) $M(\mu^+\mu^-)$ of $\Upsilon(1S)$ in $\Upsilon(1S) \to \mu^+\mu^-$ decay.

Figure 3.3: $M(e^+e^-/\mu^+\mu^-)$ for $\Upsilon(1S)$

Recoil Mass Comparison

We select $\Upsilon(1S)$ mass from 9.0 to 9.7 GeV/c^2. For recoil mass, for ee we apply a cut 9.45 GeV/c^2 $< M_{\pi\pi}^{recoil} <$ 9.468 GeV/c^2 and for $\mu\mu$ we apply a cut 9.453 GeV/c^2 $< M_{\pi\pi}^{recoil} <$ 9.47 GeV/c^2. These cuts were used in order to have more purity in the signal (i.e. to reduce the self cross feed component or a poorly reconstructed signal).

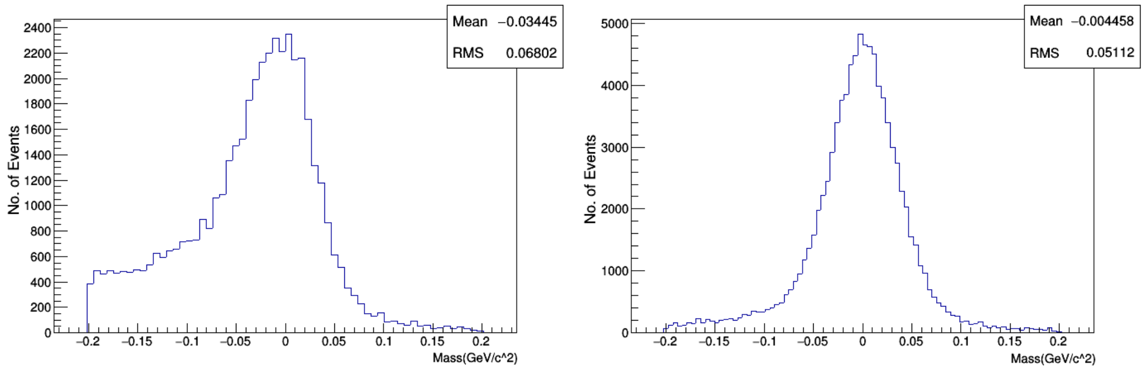

(a) δM distribution for $\Upsilon(1S)$, where $\Upsilon(1S) \to e^+e^-$.

(b) δM distribution for $\Upsilon(1S)$, where $\Upsilon(1S) \to \mu^+\mu^-$.

Figure 3.4: δM distribution for $\Upsilon(1S)$

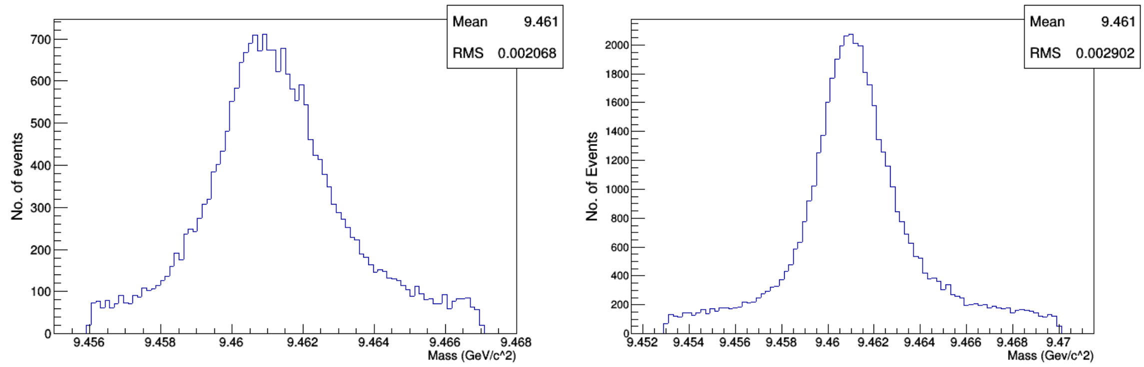

(a) $M_{\pi\pi}^{recoil}$ distribution for $\Upsilon(2S) \to \Upsilon(1S)\pi\pi$, where $\Upsilon(1S) \to ee$.

(b) $M_{\pi\pi}^{recoil}$ distribution for $\Upsilon(2S) \to \Upsilon(1S)\pi\pi$, where $\Upsilon(1S) \to \mu\mu$.

Figure 3.5: Recoil Mass distribution

3.5.2 $\Upsilon(2S) \to \Upsilon(1S)\pi\pi$ decay mode

The reconstruction of $\Upsilon(1S)$ is done through their decays to e^+e^- and $\mu^+\mu^-$. Subsequently, reconstruction of $\Upsilon(2S)$ is done by combining,

$$\Upsilon(2S) \to \Upsilon(1S)[\to e^+e^-]\pi^+\pi^- \tag{3.6}$$

$$\Upsilon(2S) \to \Upsilon(1S)[\to \mu^+\mu^-]\pi^+\pi^- \tag{3.7}$$

We select $\Upsilon(2S)$ mass from 9.5 to 10.5 GeV$/c^2$. The Fig.3.6 shows the invariant mass distribution of $\Upsilon(2S)$ for both e^+e^- and $\mu^+\mu^-$.

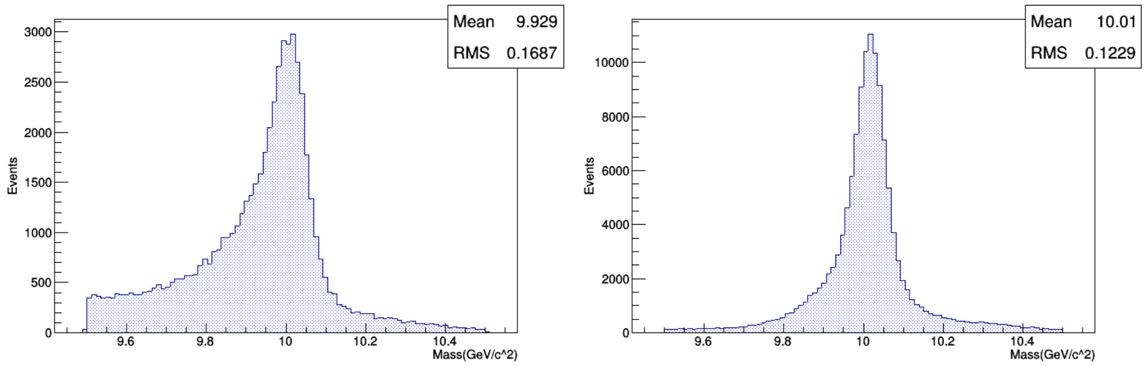

(a) $M(\ell\ell\pi\pi)$ distribution for $\Upsilon(2S) \to \Upsilon(1S)\pi^+\pi^-, \Upsilon(1S) \to e^+e^-$ decay mode.

(b) $M(\ell\ell\pi\pi)$ distribution for $\Upsilon(2S) \to \Upsilon(1S)\pi^+\pi^-, \Upsilon(1S) \to \mu^+\mu-$ decay mode.

Figure 3.6: $M(\ell\ell\pi\pi)$ distribution for $\Upsilon(2S)$.

3.5.3 Kinematical variables

To identify the $\Upsilon(2S)$, two kinematical variables are used: Invariant mass (M($\ell\ell\pi\pi$)) and Energy difference (ΔE) (eq. 3.2). Here E_{beam} is the beam energy in the center of mass (CM) frame and $E^{CM}_{\Upsilon(2S)}$ is the energy of $\Upsilon(2S)$ in center of mass (CM) frame. After this we have plotted the δM variable in Fig. 3.8 to show deviation of the invariant mass of $\Upsilon(2S)$ from the nomial mass.

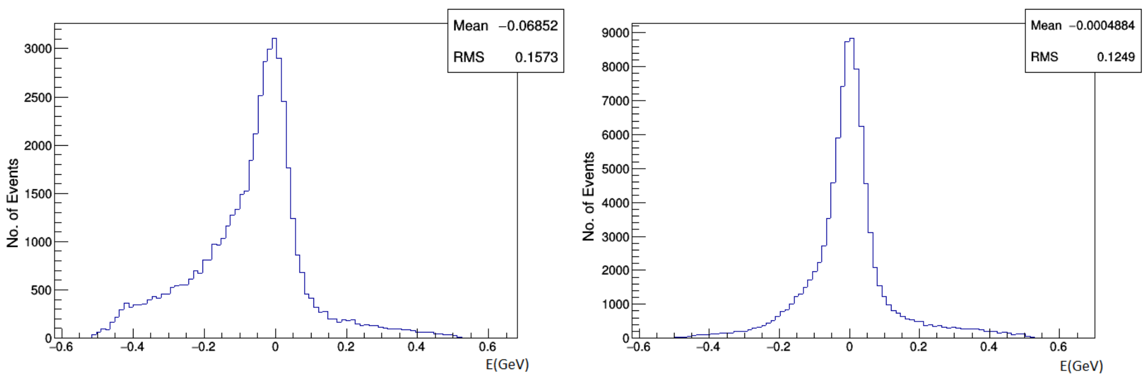

(a) ΔE distribution for $\Upsilon(2S) \to \Upsilon(1S)(\to e^+e^-)\pi^+\pi^-$

(b) ΔE distribution for $\Upsilon(2S) \to \Upsilon(1S)(\to \mu^+\mu^-)\pi^+\pi^-$

Figure 3.7: ΔE distribution for the signal MC

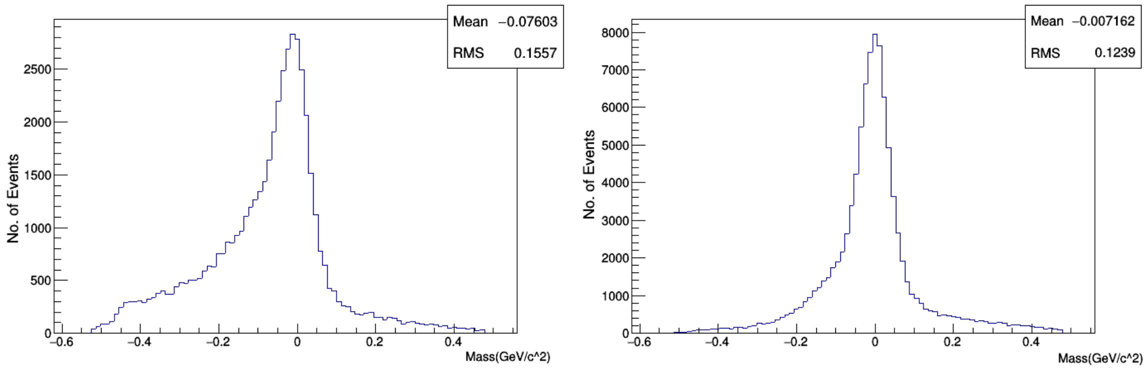

(a) δM distribution for $\Upsilon(2S) \to \Upsilon(1S)\pi\pi$, where $\Upsilon(1S) \to e^+e^-$.

(b) δM distribution for $\Upsilon(2S) \to \Upsilon(1S)\pi\pi$, where $\Upsilon(1S) \to \mu^+\mu^-$.

Figure 3.8: δM distribution for $\Upsilon(2S)$

3.6 Study of $\Upsilon(1S) \to \tau^+\tau^-$

For τ reconstruction, we have three pions and one neutrino in our decay channel, $\tau \to \pi\pi\pi\nu_\tau$. We select τ mass from 1.0 to 3.0 GeV/c^2. We also have a neutrino in the decay channel during the reconstruction part of the tau. The missing neutrino results in difficulty while reconstructing the tau mass. Fig. 3.10 shows the invariant mass of τ particle after kinematic fitting. 1 Million signal MC was generated and the

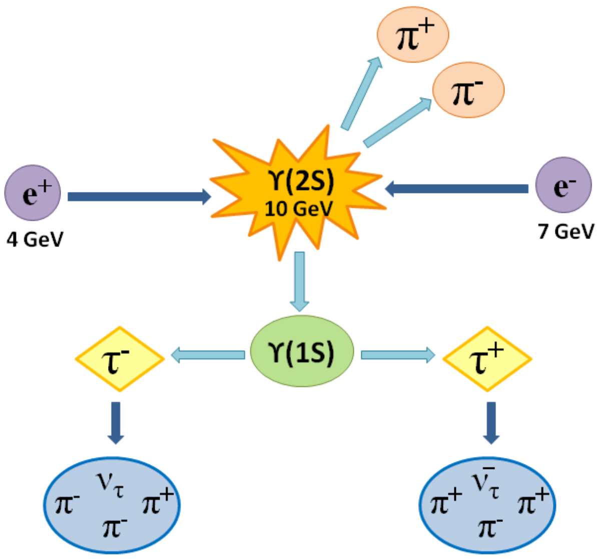

Figure 3.9: Schematic depicting $\Upsilon(2S) \to \Upsilon(1S)\pi\pi$, where $\Upsilon(1S) \to \tau^+\tau^-$ decay.

events were reconstructed. We got different values for event efficiency and tau mass by using different fitting methods from which we chose vertexTree for further studies.

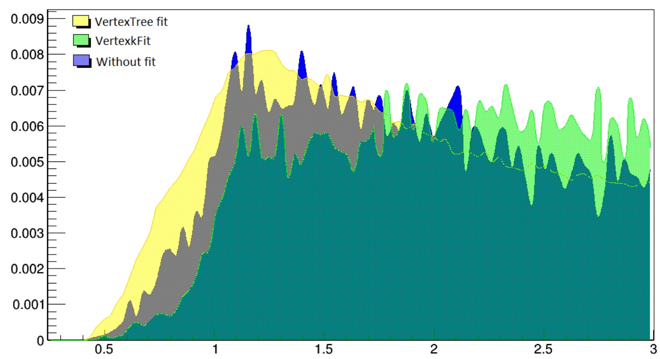

Figure 3.10: Invariant mass comparison for τ in $\Upsilon(2S)$ $\rightarrow\Upsilon(1S)(\rightarrow \tau\tau)\pi^+\pi^-$,$\tau \rightarrow \pi\pi\pi\nu_\tau$ decay mode.

1 Million signal MC was generated and the events were reconstructed. We got different values for event efficiency and tau mass by using different fitting methods from which we chose vertexTree for further studies.

3.6.1 TreeFitter

The TreeFitter is a global fitting tool to simultaneously fit an entire decay chain. It tries to optimise the best decay vertex positions and momenta for the given decay hypothesis. Final state particles will be constrained to their masses, meaning no energy is extracted from the fit but PDG-mass and momentum measurement are used to determine it (same as track fitting procedure). The fit extracts the 4-momenta ($\rightarrow$ including energy) and decay vertex positions of intermediate particles. Fig. 3.11 shows the invariant mass distribution for τ after truth matching.

3.6.2 $\Upsilon(2S)$ & $\Upsilon(1S)$ reconstruction from $\tau^+\tau^-$

The Fig. 3.12 shows the mean peak values for invariant mass and recoil mass for $\Upsilon(1S)$. Comparing the values nomial mass [Canetti 14] (i.e. 9.4 GeV/c^2) we observe a shift in peak value when is comes to invariant mass which is not the case with recoil mass.

The shift in the mean invariant mass can be because of the presence of a neutrino

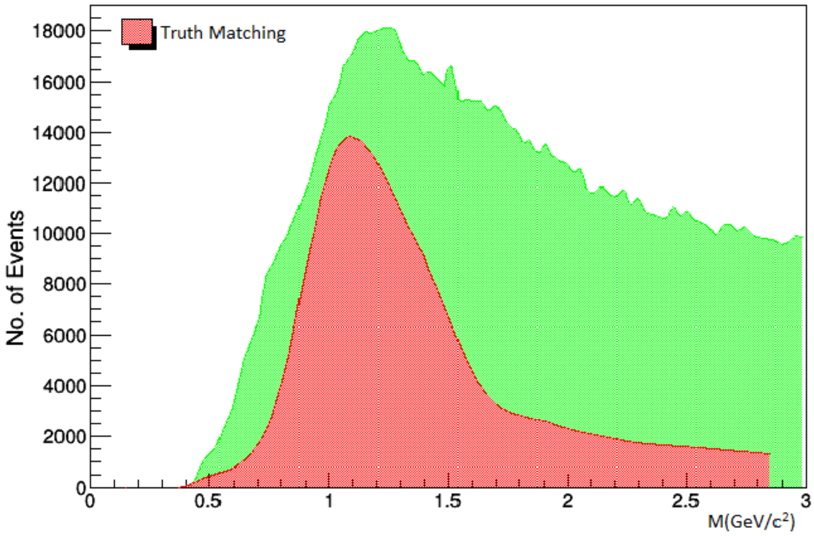

Figure 3.11: Invariant mass of τ after performing the vertex fit. Red color shows the truly reconstructed events, while the green color shows the fake events (which come from the cross feed).

while reconstruction. The missing neutrino leads to the poor reconstruction of $\Upsilon(1S)$, leading to poor mass and resolution of the reconstructed invariant mass distribution of the $\Upsilon(1S)$ and $\Upsilon(2S)$.

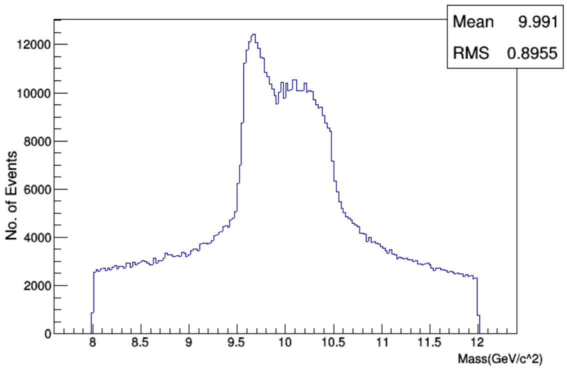

(a) $M(\tau\tau\pi\pi)$ for $\Upsilon(2S)$ decay

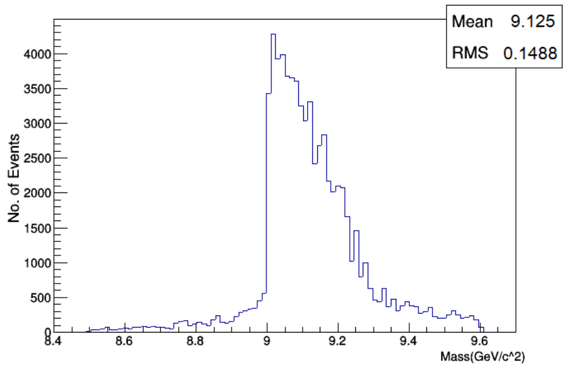

(b) $M(\tau\tau)$ for $\Upsilon(1S)$ decay

Figure 3.12: Reconstructed invariant mass for $\Upsilon(2S)$ and $\Upsilon(1S)$ for $\Upsilon(2S) \to \Upsilon(1S)(\to \tau\tau)\pi^+\pi^-$ decay mode.

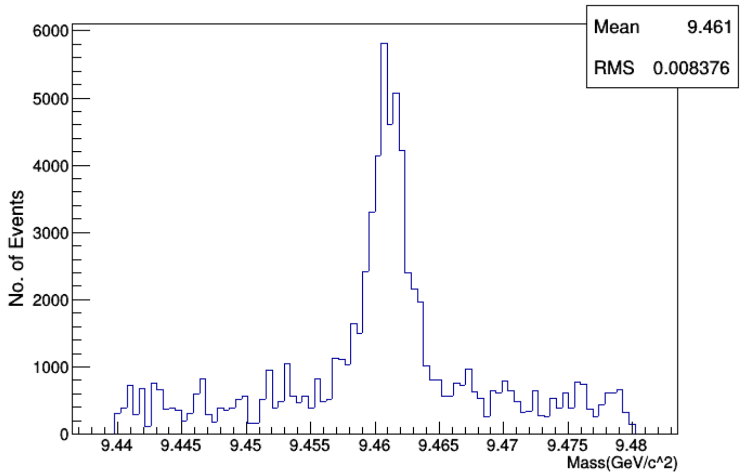

Figure 3.13: $M_{\pi\pi}^{recoil}$ distribution in $\Upsilon(2S) \to \Upsilon(1S)(\to \tau\tau)\pi^+\pi^-$ decay mode.

As seen from the Fig. 3.13, the Mrecoil peaks at the $\Upsilon(1S)$ and the resolution is much better than simple invariant mass. In order to select the $\Upsilon(1S)$ candidates, we apply the cut 9.42 GeV/c^2 $< M_{\pi\pi}^{recoil} <$ 9.5 GeV/c^2. The only downside is that, one can't distinguish whether this $\Upsilon(1S)$ is from ee, $\mu\mu$ or $\tau\tau$. In order to do so, one can further utilize the invariant mass of τ and $\Upsilon(1S)$ to identify the signal of interest. Missing Energy can also be used for such analysis. We need to study missing energy in details to do so.

Chapter 4

Missing Energy Analysis

The Belle II experiment offers unique capabilities to study the e^-e^+ decays with neutrinos in the final state, with respect to experiments at hadron colliders. The machine is designed for an instantaneous luminosity of 8 x 10^{35} $cm^{-2}s^{-1}$, and the experiment is expected to accumulate a data sample of about 50 ab^{-1} in five years of running. With this amount of data, decays sensitive to physics beyond the Standard Model can be searched for with unprecedented sensitivity. The Belle II detector is capable of high reconstruction efficiencies for both charged and neutral particles. These features allow the full reconstruction of Υ meson.

4.1 Analysis strategy

Semileptonic and leptonic decays have at least one neutrino in the final state, which escapes the detector undetected. This is similar to our study where we have one neutrino in each tau reconstruction. Leptonic decays or other B meson decays with missing energy can be measured at the B factories, due to the unique experimental conditions: known production process of e^+e^- pairs and the fact that the detector encloses the interaction region almost hermetically. These two properties allow us to infer the energy and the 4-momentum of undetected particles, such as neutrinos, from measured momenta and energies of all other particles produced in the e^+e^- collision (except for the neutrino) and imposing energy-momentum conservation.

4.2 Search for $\Upsilon(1S)$ using $\tau \to \pi\pi\pi\nu_\tau$

Our interest lies in the $\tau \to \pi\pi\pi\nu_\tau$ channel that has a branching fraction; (BR 9.80 ± 0.05)%

$$\Upsilon(2S) \to \Upsilon(1S)\pi^+\pi^-, \Upsilon(1S) \to \tau^+\tau^- \tag{4.1}$$

$$\tau^+ \to \pi^+\pi^-\pi^+\bar{\nu_\tau}, \tau^- \to \pi^+\pi^-\pi^-\nu_\tau \tag{4.2}$$

The reconstructed decay chain gives us the energies of all the constituent particles and their mother particles; except neutrino. In complete decay chain we have eight π; six from $\Upsilon(1S)$ and two from $\Upsilon(2S)$. We have all information about energy and momentum of the particles involved. The Missing Energy, $E_{missing}$, is given by,

$$E_{missing} = E_{\Upsilon(2S)} - (E_{\pi^+\pi^-\pi^+\pi^-\pi^-\pi^+} + E_{\pi^+\pi^-}) \tag{4.3}$$

As the final decay state include eight pions, there is a strong possibility that these pions may get misinterpreted or mismatched. In order to check for the true candidates and see how the distribution will look for the correct combination, we used the mother id of pion and select the only pions those are coming from $\Upsilon(1S)$.

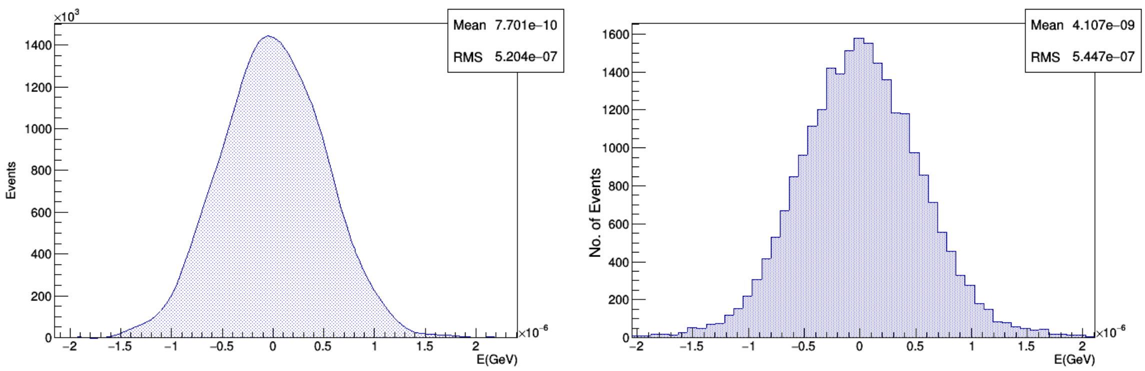

(a) $E_{missing}$ for signal.

(b) $E_{missing}$ for signal with truth-match.

Figure 4.1: $E_{missing}$ for signal

4.3 Search for $\Upsilon(1S)$ from $\tau^\pm \to \pi^0\pi^0\pi^\pm\nu_\tau$

In order to check the missing energy distribution we choose another decay channel in which τ goes to $\pi^0\pi^0\pi^\pm\nu_\tau$ with a branching fraction of 9.48 ± 0.10 %. One million events were generated for the decay channel. For recoil mass in $M_{\pi\pi}^{recoil}$ distribution we apply a cut 9.00 GeV/c^2 < $M_{\pi\pi}^{recoil}$ < 9.7 GeV/c^2 and 60% of the crossfeed will be removed. Fig. 4.3 shows the Missing energy plot.

$$\Upsilon(2S) \rightarrow \Upsilon(1S)[\rightarrow \tau^+\tau^-]\pi^+\pi^-, \tau^\pm \rightarrow \pi^0\pi^0\pi^\pm\nu_\tau \tag{4.4}$$

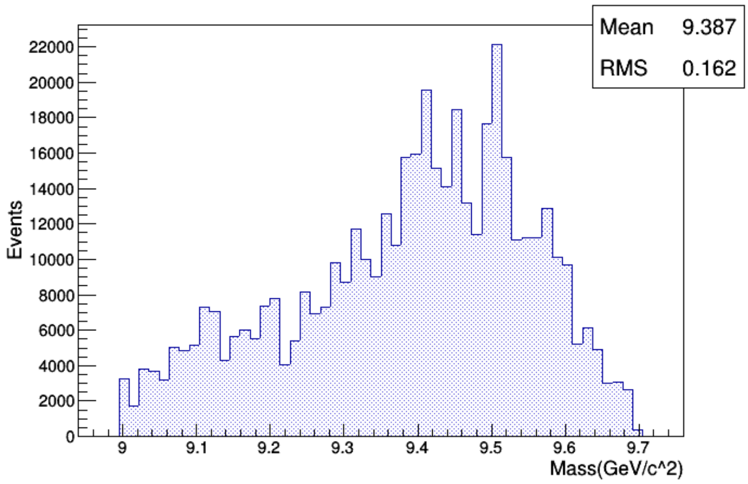

Figure 4.2: $M_{\pi\pi}^{recoil}$ distribution for $\Upsilon(2S) \rightarrow \Upsilon(1S)[\rightarrow \tau^+\tau^-]\pi^+\pi^-,\tau^\pm \rightarrow \pi^0\pi^0\pi^\pm\nu_\tau$ decay mode.

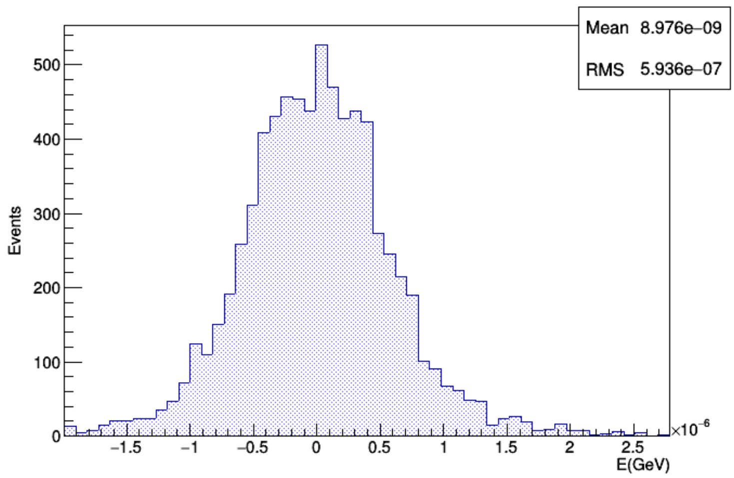

Figure 4.3: E_{Missing} distribution for the $\Upsilon(2S)$ $\rightarrow \Upsilon(1S)[\rightarrow \tau^+\tau^-]\pi^+\pi^-,\tau^\pm \rightarrow \pi^0\pi^0\pi^\pm\nu_\tau$ decay mode for the signal MC sample.

4.4 Study for $\Upsilon(1S)$ from $\tau^{\pm} \to \pi^0\pi^{\pm}\nu$

In order to check the Missing Energy distribution we choose another decay channel in which τ goes to $\pi^0\pi^{\pm}\nu$ with a branching fraction of 25.93 ± 0.09 %. One million events were generated for the decay channel (4.5) and plot the $M_{\pi\pi}^{recoil}$ distribution and missing energy for the same.

$$\Upsilon(2S) \to \Upsilon(1S)[\to \tau^+\tau^-]\pi^+\pi^-, \tau^{\pm} \to \pi^0\pi^{\pm}\nu_{\tau} \tag{4.5}$$

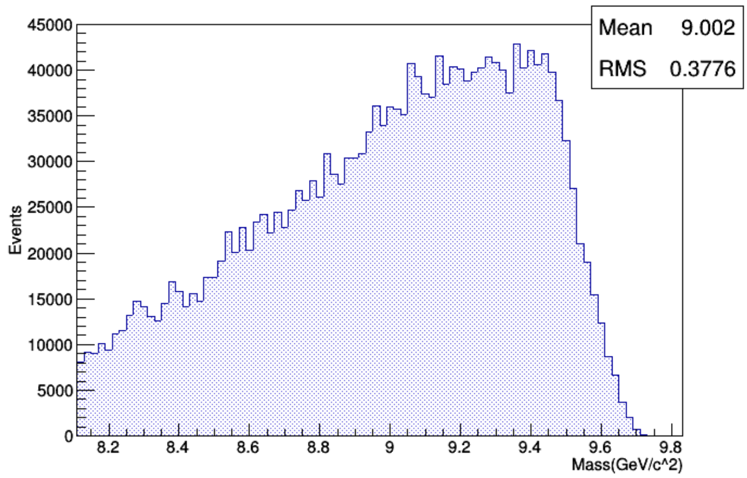

Figure 4.4: $M_{\pi\pi}^{recoil}$ distribution for the $\Upsilon(2S) \to \Upsilon(1S)[\to \tau\tau]\pi\pi$ decay mode.

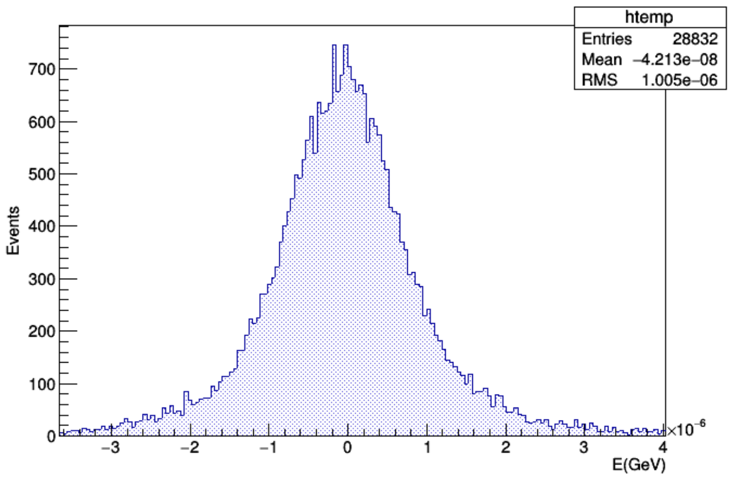

Figure 4.5: $E_{missing}$ for $\Upsilon(2S) \to \Upsilon(1S)[\to \tau\tau]\pi^+\pi^-$, where $\tau^{\pm}$ decays to $\pi^0\pi\nu_{\tau}$ decay mode.

In this chapter we've used different decay channels to compare the recoil mass distribution. The Fig. 4.2 and Fig. 4.4 show the Recoil Mass ($M_{\pi\pi}^{recoil}$) distributions for each decay channel. The initial plan was to compare Missing Energy value using a proper background simulated sample (containing all the possible $\Upsilon(2S)$ decays). However under the current circumstances, we could not generate and process the sample.

Chapter 5

Summary & Conclusions

We started this thesis with aim to reconstruct $\Upsilon(1S)$ from its τ decays. In order to do that, we first validated our MC and reconstruction on the well known $\Upsilon(1S)$ decays to ee and $\mu\mu$ modes. We start the analysis using the control samples;

$$\Upsilon(2S) \to \Upsilon(1S)\pi^+\pi^-, \Upsilon(1S)[\to ee/\mu\mu] \tag{5.1}$$

After gaining the confidence, we started with the $\Upsilon(1S)$ decays having τ in its final state. Due to the missing neutrino, this decay mode is a bit difficult.

$$\Upsilon(2S) \to \pi^+\pi^-\Upsilon(1S)[\to \tau^+\tau^-], \tau \to \pi\pi\pi\nu_\tau, \pi^0\pi^0\pi\nu_\tau, \pi^0\pi\nu_\tau \tag{5.2}$$

Reconstruction data to approximately mimic real experiments for each decay channel was used. Recoil Mass distribution and Missing Energy, in this work were most important variable due to the energy loss of neutrinos.
We generated 1 million events for each signal channel and removed the background and check the reconstruction efficiency through recoil mass distribution.
One can use the variables (recoil mass, missing energy, invariant mass) in order to distinguish the signal. It would have been interesting to compare these variables from the background and optimize the cuts (which we missed due to the COVID-19). Future work is to optimize the cuts, run on the generic background samples, use other variables and train NN on signal vs background.

Bibliography

[Adachi 18] I. Adachi, T.E. Browder, P. Križan, S. Tanaka & Y. Ushiroda. *Detectors for extreme luminosity: Belle II.* Nuclear Instruments and Methods in Physics Research Section A: Accelerators, Spectrometers, Detectors and Associated Equipment, vol. 907, pages 46 – 59, 2018. Advances in Instrumentation and Experimental Methods (Special Issue in Honour of Kai Siegbahn).

[Canetti 14] Laurent Canetti, Marco Drewes & Björn Garbrecht. *Probing leptogenesis with GeV-scale sterile neutrinos at LHCb and Belle II.* Physical Review D, vol. 90, no. 12, page 125005, 2014.

[Kuhr 18] Thomas Kuhr, Christian Pulvermacher, Martin Ritter, Thomas Hauth & Nils Braun. *The Belle II Core Software.* Jul 2018.

[Li 15] Yao Li. *Analysis on $B^{\pm} \to \pi^{\pm}\pi^{+}\pi^{-}$.* PhD thesis, Virginia Tech., 2015.

[Nakamura 18] K Nakamura, ST Petcov*et al.* *Neutrino masses, mixing, and oscillations.* 2018.

[S. Patra 0] Karim Trabelsi S. Patra Vishal Bhardwaj. https://belle.kek.jp/secured/belle_note/gn1549/bn1549.pdf, 2020 (January 30, 2020).

Appendix A

Appendix

A.1 Decay files for signal generation

For *ee*

Alias $\Upsilon(1S)$ Upsilon

Alias $\Upsilon(2S)$ Upsilon(2S)

Decay Upsilon(2S)sig

1.000 Upsilonsig pi+ pi- PHOTOS VVPIPI;

Enddecay

Decay Upsilonsig

1.000 e+ e- PHOTOS VLL;

Enddecay

End

For $\mu\mu$

Alias $\Upsilon(1S)$ Upsilon

Alias $\Upsilon(2S)$ Upsilon(2S)

Decay Upsilon(2S)sig

1.000 Upsilonsig pi+ pi- PHOTOS VVPIPI;

Enddecay

Decay Upsilonsig

1.000 mu+ mu- PHOTOS VLL;

Enddecay

End

For $\pi\pi\pi\nu$

Alias $\Upsilon(1S)$ Upsilon

Alias $\Upsilon(2S)$ Upsilon(2S)

Decay Upsilon(2S)sig

1.000 Upsilonsig pi+ pi- PHOTOS VVPIPI;

Enddecay

Decay Upsilonsig

1.000 tau+ tau- PHOTOS VLL;

Enddecay

Decay tau+

0.09320 pi+ pi- pi+ $\bar{\nu_\tau}$ TAUHADNU $-0.1080.7750.1491.3640.4001.230.4$;

Enddecay

Decay tau-

0.09320 pi- pi- pi+ ν_τ TAUHADNU $-0.1080.7750.1491.3640.4001.230.4$;

Enddecay

End

Index